UNCLASSIFIED

# A MULTI-LAYER SILICON NEUTRON DETECTOR FOR DISCRIMINATION (U)*



R. Schulte, E. Kamykowski, A. Celona, and M. Kesselman
Grumman Corporate Research Center
Bethpage, NY 11714-3580

ABSTRACT. (U) A neutron detector based on a multi-layer silicon proton recoil detection scheme is under development. The neutron detector uses polyethylene sheets as a neutron convertor and a stack of three silicon wafers to detect the recoiling protons. The multi-layer silicon detector features variable threshold for low energy neutrons, nominal $2\pi$ directional response, and low sensitivity to gamma rays. Pulse processing electronics has been developed to analyze signal events in real time to determine the direction of the incoming neutron. The multi-layer silicon sensor system has been tested under various neutron and gamma radiation conditions. The sensor efficiency and angular response have been measured for 15 MeV monoenergetic neutrons.

## 1. INTRODUCTION (U)

(U) A key element of the Neutral Particle Beam (NPB) discrimination is the sensor required to detect the neutron emissions from the NPB irradiated target. Due to the nature of the background radiation environment, an operational sensor must satisfy top level requirements of directionality, energy thresholding for neutrons, and low sensitivity to gamma radiation. The directional capability of the sensor will reduce the background from the earth's neutron albedo and some cosmic ray induced activity; the energy threshold will eliminate the background from the low energy neutrons from a fission pulse; likewise, the gamma sensitivity should be significantly low so that delayed gammas from a fission pulse do not compromise the operation of the sensor.

(U) We have been developing a neutron sensor based on a Multi-Layer Silicon (MLS) detection system that meets all the requirements of a candidate sensor. In this paper we report on the development and testing of a MLS sensor unit. A brief description of the MLS sensor system is presented along with a discussion of the experimental tests and the performance of the detector under various irradiation conditions.

## 2. MLS NEUTRON SENSOR SYSTEM (U)

### 2.1 The MLS Detector (U)

(U) We have configured a basic MLS detector to demonstrate its characteristics of energy thresholding and directionality. The configuration used is shown in Figure 1 and consists of three partially depleted silicon (Si) wafers adjacent to a polyethylene ($CH_2$) convertor. The $CH_2$ layer serves as a scattering medium for incoming neutrons

*This work was supported by the U.S. Army Strategic Defense Command under Contract No. DASG60-90-C-0039

UNCLASSIFIED

producing recoil protons in the process. The high-energy protons emerge from the $CH_2$ convertor layer and are detected by the Si stack to produce a proton recoil detector. The key to the operation of the MLS detector is the orientation of the Si wafers within the stack. The first wafer is oriented so that its dead layer is facing the front and the depletion (or active) zone faces the rear. This is the wafer that is responsible for the thresholding capability. By lowering the bias voltage applied to the detector, we increase the energy threshold since protons of higher energy are needed to penetrate through the increased dead layer into the depletion zone. This technique produces a continuously variable threshold that is adjusted by merely raising or

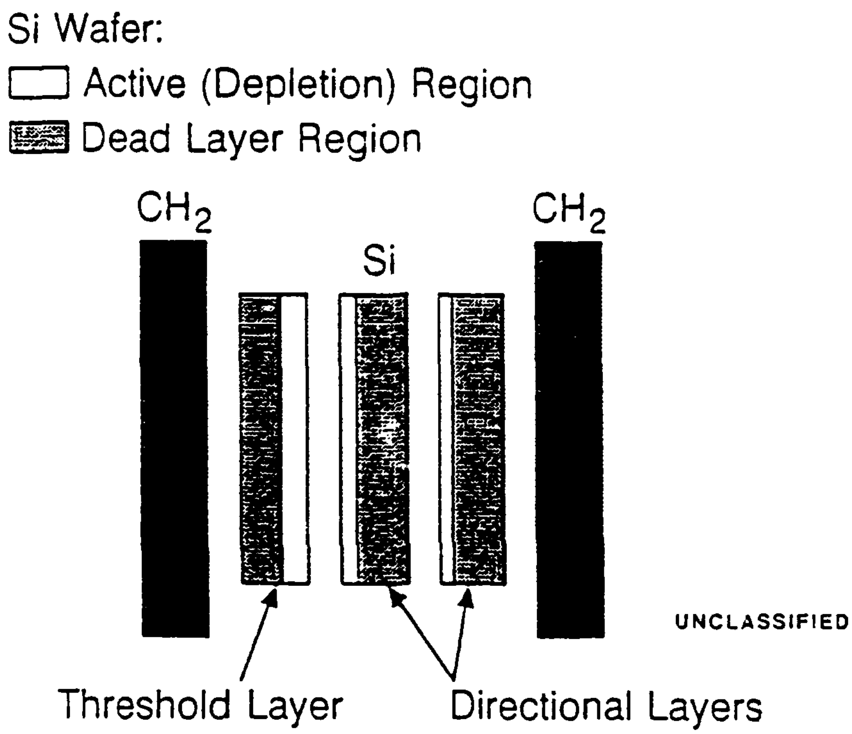


Figure 1. (U) Schematic diagram of the cross sectional view of the detection plane of a Multi-Layer Silicon sensor.

lowering the bias voltage applied to the detector. The second and third wafers in the stack produce the directional characteristic of the detector. For these wafers, the depletion zones are closely matched by bias voltage settings and are both facing the front of the detector. The depletion zones are fixed at an appropriate thickness so that sufficient energy is deposited by a proton to exceed the setting of the lower level discriminator which is set to eliminate the gamma energy deposition. A proton passing through the stack deposits more energy per unit length as its energy decreases. This fact is used to determine the direction of the recoiling proton by comparing the energy deposited in the second and third wafers of the stack. If the energy deposited in the third layer exceeds that in the second layer, the recoil proton is passing from the front to the rear of the detector and vice versa. This logic is easily incorporated into pulse processing electronics to determine the direction of the recoil proton.

(U) Note that the third wafer has its dead layer facing the rear $CH_2$ layer thus imposing a fixed threshold to recoil protons coming from the rear of the stack. A unique feature of the MLS sensor is that the proton recoils from the low energy neutrons are stopped in dead layers, thus eliminating sub-threshold events and thereby reducing electronic pile-up and drift effects that a high count rate background might otherwise create.

(U) In the present investigation we have used 5.08cm x 5.08cm (25.8cm$^2$ active area) silicon wafers that are segmented into four quadrants (nominally 1 in. x 1 in.). The detectors are nominally 300µm thick and capable of full depletion at applied bias voltages of 30 to 60 volts. The MLS detector is configured with three of these Si wafers with ultra-high molecular weight (UHMW) polyethylene sheets mounted front and rear.

(U) At this phase of the sensor development we selected 300µm thick Si wafers over the more conventional 500µm to gain added flexibility in testing the MLS concept. Although higher neutron energy thresholds can be achieved with 500µm thick Si, with the 300µm thick Si we have interposed thin aluminum filters between the $CH_2$ and the first Si wafer to achieve the same dynamic range as the 500µm Si.

## 2.1 MLS Electronics (U)

(U) The pulse processing electronics consists of an analog and a digital stage for real-time event processing. The analog board contains inputs for four separate detectors each consisting of three wafers in a stack. Each input consists of a LeCroy HQV110 preamplifier followed by an amplifier and shaping circuit. The digital board contains the peak-detect circuit, the comparators and the programmable logic array. There are only three outputs on the digital board, i.e., the event present, valid event and invalid event. A valid event is one for which the logic has determined the recoil proton passed from front to rear of the detector stack; for an invalid event the proton passed from the rear to the front of the detector.

(U) A signal occurring in any of the three wafers of the stack will trigger the system and the event is analyzed based on the signals or lack of signal from the three wafers. A discriminator level is set at each input to eliminate noise and unwanted pulses due to gamma interactions. The signals are amplified and shaped for acceptance by the peak detect circuits which establish the pulse heights. The coincident pulses that occur in the second and third wafers of the stack pass into a comparator circuit to determine which wafer has produced the greater pulse height. The logic array (PAL) has been programmed to categorize each event as valid or invalid based on the pulses from each of the three input channels. An event, for example, that does not trigger the first channel of the stack is designated as an invalid event because the event could not have originated at the front of the detector stack. Likewise, an event that does not trigger the third channel is designated as valid since it could not have originated at the rear of the detector. Only when an event triggers all three channels does the result of the pulse height comparison in channels two and three come into play in the designation of the event as valid or invalid. All possible event combinations are coded to produce the most likely designation for each event. A buffer amplifier

produces the output pulses to increment counters for the event present and the event designation. Real-time analysis is a requirement for an operational sensor to assure that the discrimination time is kept to a minimum.

## 3. SENSOR TESTS AND RESULTS (U)

(U) Initially, functional tests were conducted to evaluate the pulse processing circuitry and validate the logic. The bare MLS detector stack (without $CH_2$) was irradiated with high energy protons (Ep=13.5 MeV) incident on the front of the detector. The protons were generated with the $^2H(^3He,p)^4He$ reaction at $E_{3He}$=1.2 MeV using the 4 MV Grumman Van de Graaff accelerator. Fully 99.3% of the events were correctly designated as valid events. The detector was then reversed so the protons were incident on the rear of the detector stack, resulting in 97.5% of the events correctly identified as invalid events.

(U) The Grumman Van de Graaff accelerator was also used to generate neutrons with the $^3H(^2H,^4He)n$ reaction. To characterize the neutron flux generated, we measured the neutron spectrum at 0 degrees with respect to the incoming deuteron beam using a BC501 liquid scintillator. Upon deconvolution of the spectrum using the FORIST code, we obtained nominal 15 MeV neutrons at a flux of approximately $2.2 \times 10^3$ n/cm$^2$•s as shown in Figure 2.

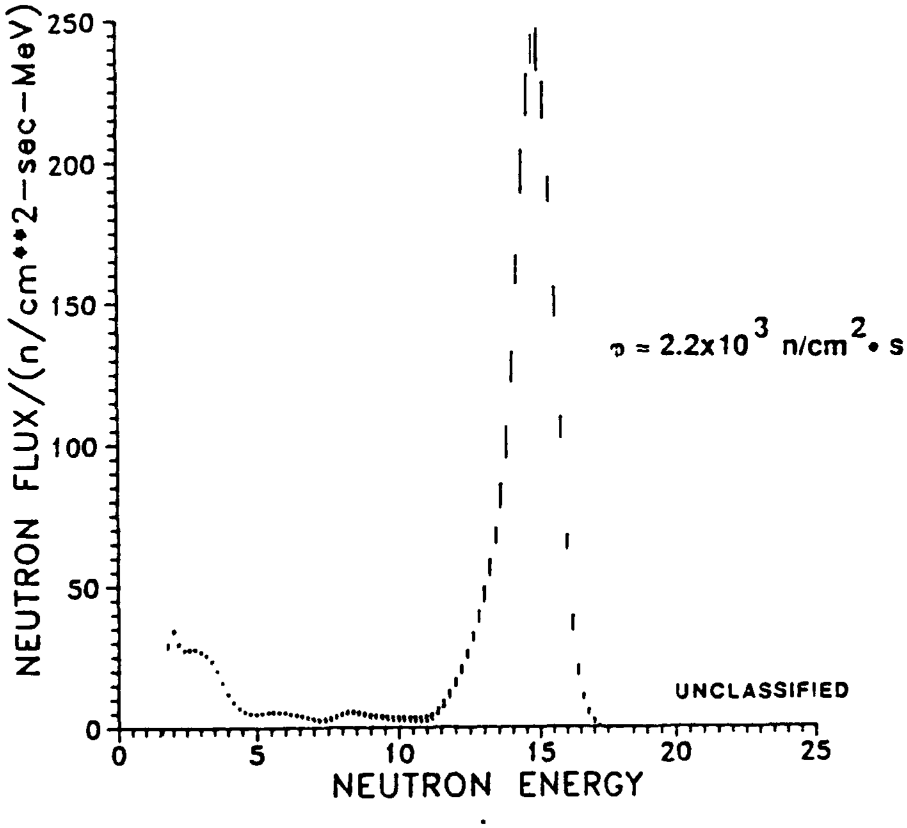


Figure 2. (U) Spectrum of 15 MeV neutrons used in the MLS sensor tests. The spectrum was deconvolved using the FORIST code.

(U) The MLS neutron detector unit was mounted in an evacuated test chamber with a thin aluminum end plate. A small silicon surface barrier detector with a 1.5mm thick polyethylene convertor in front was situated next to the MLS detector to serve as a neutron monitor.

(U) The spectral response of the first wafer in the silicon stack is shown in Figure 3 for two different energy threshold settings. The MLS sensor was irradiated with 15 MeV neutrons and a gamma flux of $2x10^6$ $\gamma/cm^2 \bullet s$ from a $^{137}Cs$ source situated at the front of the sensor. The portion of the spectrum due to only gammas incident on the sensor is shown by the dashed line in the figure. The gamma ray contribution to the spectrum is at low energy due to the thin depletion regions of the silicon wafers and the fact that specific energy loss for electron in silicon is 15 to 20 times smaller than for protons of the same energy. No evidence of pile-up exists at this gamma flux level so a discriminator level setting just above the edge of the gamma contribution would eliminate the gamma influence. The broad feature at the center of the spectrum is due to proton recoils from the $CH_2$ convertor layer and the low count-rate continuum at higher channels (>240) is due to neutron interactions in the silicon. A similar set of spectral features is shown in Figure 3B for the higher energy threshold setting (7.5 MeV). For the higher threshold, the depletion region is thinner and less energy is deposited in the first silicon wafer by the electrons and recoil protons.

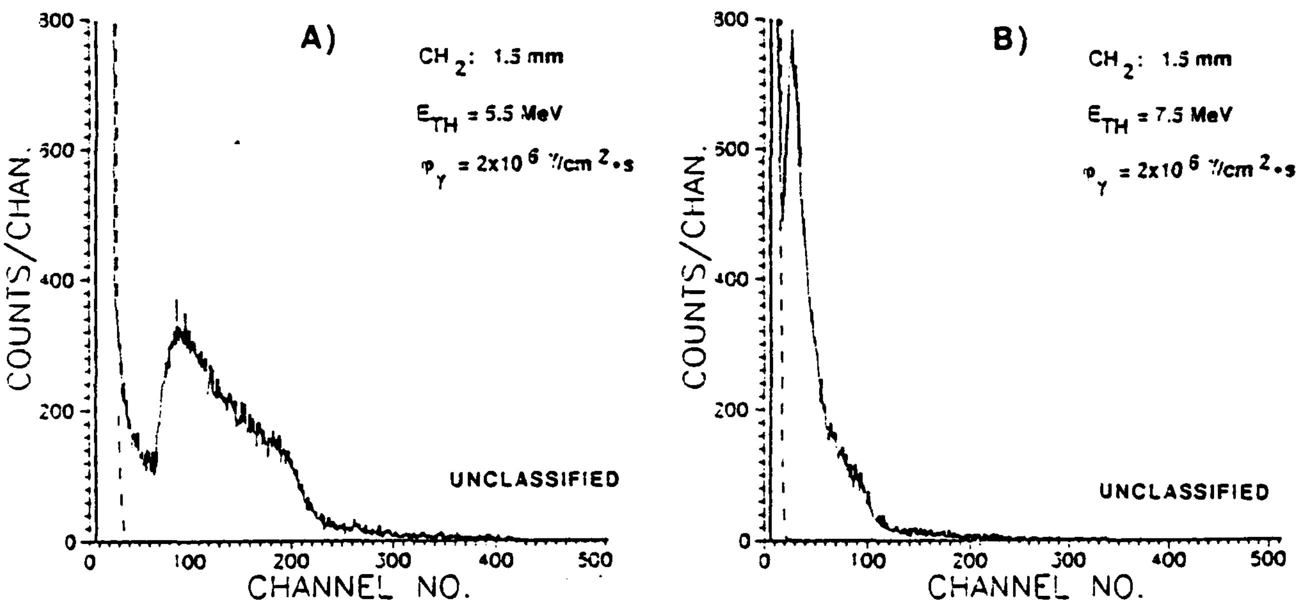


Figure 3. (U) Spectra from the first wafer of the silicon stack for two neutron energy thresholds. The response to irradiation by 15 MeV neutrons and 0.662 MeV gamma rays (dashed line) is shown.

(U) The MLS sensor efficiency for 15 MeV neutrons was measured as a function of $CH_2$ convertor thickness and neutron energy threshold. Figure 4 shows the intrinsic efficiency versus the $CH_2$ convertor thickness for the zero threshold condition (i.e., the threshold layer Si wafer is fully depleted). The data are plotted along with the calculated efficiency. The shape of the curve is nearly linear for very thin (<400μm)

$CH_2$ layers since most of the recoil protons from the 15 MeV neutrons escape the $CH_2$ layer and are detected in the Si detector. As the $CH_2$ layer becomes thicker, the fraction of recoil protons that are stopped in the polyethylene increases. When the $CH_2$ layer becomes thicker than the range of the maximum energy recoil proton that can be produced, the efficiency no longer increases with $CH_2$ thickness. Efficiency curves of these types are highly dependent on the incident neutron energy and the setting of a neutron energy threshold. The maximum efficiency for low energy neutrons is achieved with thinner $CH_2$ layers and for high energy neutrons with thicker $CH_2$ layers.

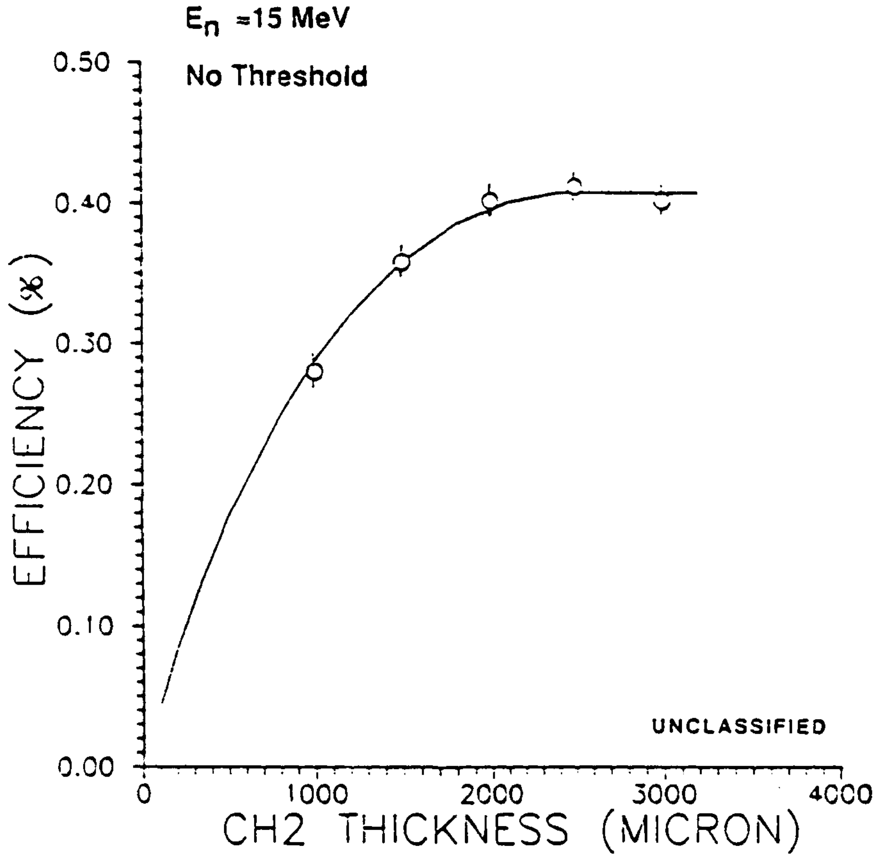


Figure 4. (U) MLS detector efficiency measurements and prediction as a function of polyethylene thickness.

(U) For a 1.5mm thick $CH_2$ layer in front of the MLS sensor we have measured the efficiency as a function of the neutron energy threshold. Figure 5 shows the results for threshold energy settings ranging from no threshold to 7.5 MeV. The efficiency at $E_{TH}$=7.5 MeV is approximately one-half that for no threshold. The intrinsic efficiency is readily calculated for a given MLS sensor configuration so we are able to determine the appropriate $CH_2$ thickness to achieve optimal efficiency for a given neutron energy or neutron energy distribution incident on the sensor.

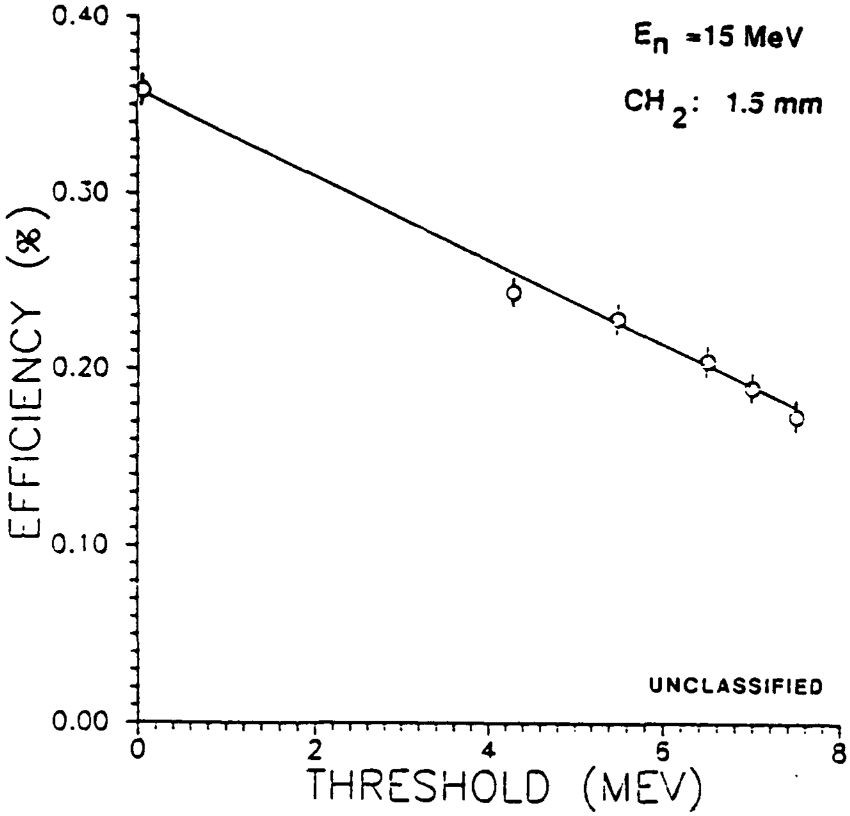


Figure 5. (U) MLS detector efficiency for 1.5mm polyethylene as a function of neutron energy threshold level.

(U) The angular response of the MLS sensor to 15 MeV neutrons has also been measured at four incident angles as shown in Figure 6. These data are the net counts from the neutron interactions in the $CH_2$ layer. The shape of the angular response matches the cosine squared function plotted in the figure (solid line). When coupled with the front-to-back directionality of the sensor, this response results in a slightly better than $2\pi$ directionality for the MLS sensor.

4. CONCLUSIONS (U)

(U) The MLS neutron sensor is based on proton recoil detection using a stack of three partially depleted silicon wafers. The depletion region can be quite thin (~100μm) so a low cost, low resistivity silicon can be used. The bias voltage requirements for the MLS sensor are typically 50 volts or less. The sensor is able to achieve a continuously variable neutron energy threshold by adjusting the applied bias voltage on the first (threshold) wafer in the stack. A key feature of the threshold capability is that

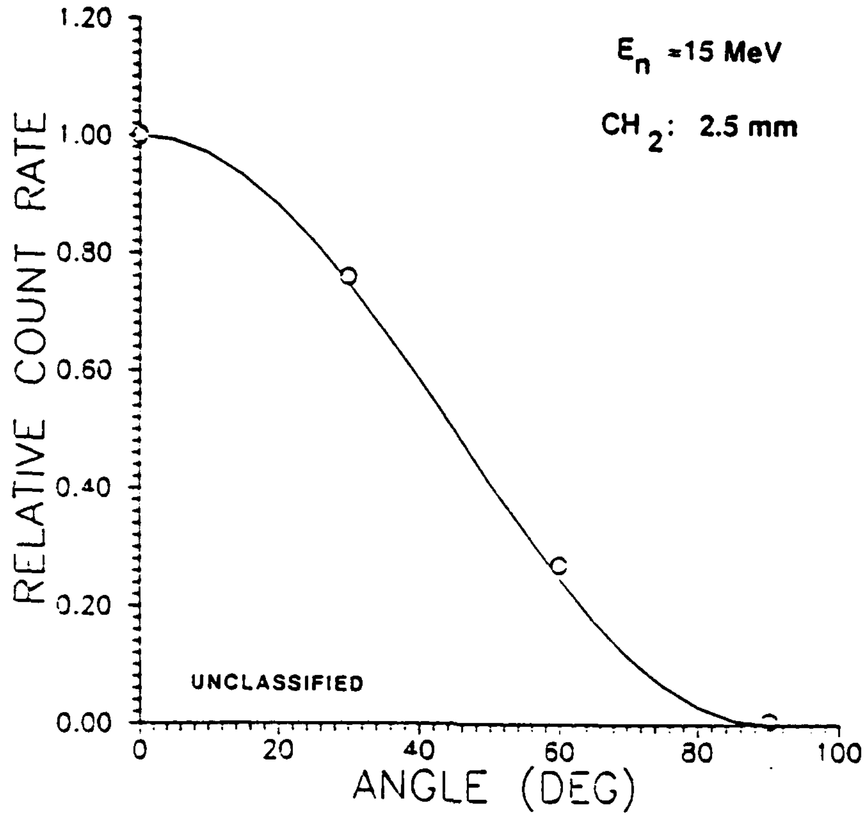


Figure 6. (U) Angular response of the MLS detector to 15 MeV neutrons follows a cosine-squared function.

subthreshold neutrons generate low energy proton recoils that are stopped in the dead layer of the sensor and cannot contribute to electronic pile-up. The directional response of the MLS sensor is nominally $2\pi$ achieved through a real-time, distributed signal processing of events in the sensor. The geometric configuration of the sensor contributes to a cosine-squared response, thus improving the angular response in the forward direction. The gamma sensitivity of the MLS sensor is reduced by using thin detection regions in the silicon wafers and imposing the required coincidence for multiple wafers in the silicon stack.

(U) In this report we have demonstrated some of the key features of the MLS sensor system. The wide range of design parameters that can be varied within the MLS sensor concept assures that a design configuration for an operational sensor is achievable.

ACKNOWLEDGEMENTS (U)

(U) We gratefully acknowledge the technical help provided by T. Kantorcik throughout the course of this study.

-DE -C
(J. Madewell)

S: 10 Jul 91

CSSD-PA (360-5b)

2 Jul 91

MEMORANDUM FOR CSSD-DE (J. Madewell), -IN-CT

SUBJECT: Request for Clearance for Public Release, Case # 91-342
Title - A Multi-Layer Silicon Neutron Detector for Discrimination
(for open publication - was presented at closed session of NPB Tech Symposium in April)

1. References:

a. USASDC Reg. No. 10-3, Command Policies, 27 Mar 86 (Chap 10).

b. AR 360-5, Public Information, 31 May 89 (Chap 9).

c. AR 380-5, DA Information Security Program, 25 Feb 88.

d. AR 530-1, Operations Security, 1 Apr 91.

e. USASDC BMD Classification Guide, 3 Jul 89, or approved security classification guides for individual project offices or SDI programs.

f. DoD Directive 5230.24, 18 Mar 87, subject: Distribution Statements on Technical Documents.

g. DoD Directive 5230.25, 6 Nov 84, subject: Withholding of Unclassified Technical Data from Public Disclosure.

2. Request:

a. Review of subject material (encl 1) which reflects work under USASDC Contract No. DASG60-90-C-0039 or MIPR ______ .

b. Completion of Request for Review Form (encl 2).

c. Return of enclosures 1 and 2 to CSSD-PA, ATTN: Gerda Sherrill, tel. 5-3888, NLT 10 Jul 91 .

2 Encls

for Gerda M. Sherrill
EDWARD H. VAUGHN
Chief, Public Affairs Office

**REQUEST FOR REVIEW FORM**

**CASE #:** 91-342 **REVIEW MATERIAL:** Silicon Neutron Detector... **DATE:** 2 Jul 91

1. Should the review be accomplished by a USASDC-Huntsville operational or staff element other than those listed as addressees on cover memorandum or by another Government activity?
______ YES. __X__ NO.

If YES, by whom? ____________________

2. Against which topic(s) of the USASDC BMD Classification Guide (or approved security classification guides for individual project offices) or other guidance was this material reviewed?

SDIO/TND Neutral Particle Beam Security Classification Guide 1 APR 91

3. Does subject information require protection under any of the provisions of the guidance cited in para 1 of the cover memorandum?
______ YES. __X__ NO.

If YES, cite the specific guidance and correct the material, if possible, to permit public release.
Please provide recommendations under para 8 (Comments) below.:

4. Does this material:
   a. Contain export-controlled technical data? ___ YES. _X_ NO.
   b. Describe militarily critical technology? ___ YES. _X_ NO.
If YES, indicate which limited distribution should be assigned to the document (consult DoD Dir 5230.24): ____________________

5. Could release of this material to potential adversaries of the USA be detrimental to current U.S. research and development technologies?
______ YES. __X__ NO.

6. Classification (please check either one):

______ The material is determined to be CLASSIFIED (or sensitive).

__X__ The material is determined to be UNCLASSIFIED (and releasable).

7. Reviewing official(s):

NAME, TITLE, OFFICE SYMBOL: J Michael Madewell Electronics Eng. CSSD-DE-C

SIGNATURE, DATE (Technical Monitor): J. Michael Madewell

SIGNATURE, DATE (Office OPSEC POC): ____________________

8. Comments:

Encl 2 CSSD-PA